ELSEVIER

International Journal of Heat and Fluid Flow 20 (1999) 158–165

International Journal of HEAT AND FLUID FLOW

Influence of mainstream flow history on film cooling and heat transfer from two rows of simple and compound angle holes in combination

B.Y. Maiteh [a], B.A. Jubran [b,*]

[a] *Department of Mechanical Engineering, New Jersey Institute of Technology, NJ, USA*
[b] *Department of Mechanical Engineering, University of Jordan, Amman, Jordan*

Received 2 August 1997; accepted 31 October 1998

Abstract

This paper describes the results of an experimental investigation into the effect of the mainstream flow history on the film cooling effectiveness and the heat transfer characteristics from the combination of one row of simple angle holes and one row of compound angle holes. The mainstream flow history includes: favorable pressure gradient factors in the range -1.11×10^{-6} to $+1.11 \times 10^{-6}$ and turbulence intensity in the range 0.3–4.7%. The presence of favorable pressure gradients in the flow reduces the film cooling protection of the surfaces from both compound angle holes or combination of simple and compound angle holes, while the presence of adverse pressure gradients increases the film cooling effectiveness at low blowing rate and decreases it at high blowing rate. Increasing the turbulence intensity reduces the film cooling effectiveness from compound angle holes or combination of simple and compound angle holes. © 1999 Elsevier Science Inc. All rights reserved.

Notation

A_s	area of test surface
D	injection hole diameter
E	voltage across the heater
h	heat transfer coefficient with film cooling
h_o	heat transfer without film cooling
I	momentum flux ratio $= \rho_c U_c^2/\rho_\infty U_\infty^2$ or the electrical current
K	pressure gradient factor, $\frac{\nu}{U^2}\frac{\partial U_\infty}{\partial x}$
M	blowing rate, $\rho_c U_c/\rho_\infty U_\infty$
P	pitch distance between the holes
q	wall heat flux
Re_L	Reynolds number based on a length along the test surface
Re_D	Reynolds number of coolant based on the injection hole diameter
s	equivalent slot width
R_{cond}	thermal conduction resistance
S	streamwise distance between the holes
St_o	Stanton number without film cooling
St	Stanton number with film cooling
St_f	iso-energetic Stanton number with film cooling
T	static temperature
Tu	freestream turbulence intensity
U	streamwise mean velocity
X, x	downstream distance as measured from the leading edge of the boundary layer trip or from the downstream edge of the injection holes when used as x/D
Y, y	vertical distance from the test surface measured upward
Z, z	spanwise distance measured from the test section centerline

Greek

β	injection hole angle with respect to the test surface as projected into the spanwise/normal plane
η	adiabatic film cooling effectiveness
$\overline{\eta}$	spanwise-averaged adiabatic film cooling effectiveness
ρ	density
θ	non-dimensional coolant temperature
δ	boundary layer thickness
δ^*	boundary layer displacement thickness
ε	emissivity of the test surface
Ω	injection hole angles with respect to the test surface as projected into the streamwise/normal plane

Subscripts

aw	adiabatic wall
c	coolant at exit of injection holes
r	recovery condition
w	wall
∞	freestream

1. Introduction

Numerous experimental investigations have been conducted to study various parameters affecting film cooling and heat transfer characteristics from simple angle holes with little work on compound angle holes. These investigations include

* Corresponding author. E-mail: bassamj@iiu.edu.my.

0142-727X/99/$ – see front matter © 1999 Elsevier Science Inc. All rights reserved.
PII: S0142-727X(98)10057-7

geometrical parameters: holes and row spacings, simple injection angle holes, and operational parameters: blowing rates, boundary layer developments, pressure gradients over the blade surfaces and freestream turbulence intensity. It is interesting to note that most of these investigations especially for the mainstream flow history have been carried out for holes with simple injection angles, such as the work reported by Mehendale and Han (1992) and Bons et al. (1996), with little regarding complex shape holes. One of the important parameters which affect the characteristics of film cooling is the shape of the holes and there is a general trend now towards exploring the utilization of more complex hole shapes with particular renewed research interest in using compound angle holes such as the works of Ligrani and Mitchell (1994), Ekkad et al. (1995) and Schmidt et al. (1996). The influences of the operational parameters, namely: mainstream turbulence intensity and pressure gradients on film cooling from injection holes with complex shapes, seem to attract less attention than holes with simple shapes.

Ligrani and Mitchell (1994) studied the interactions between single embedded vortices and injectant from film cooling holes with compound angle orientations and different spanwise spacing holes in the turbulent boundary layer. Jumper et al. (1991) investigated the effects of high turbulence flow on film cooling effectiveness from a single row of 30° slant-hole injectors. It was found that increasing the Reynolds number or freestream turbulence results in an increase in the blowing ratios for optimum film cooling effectiveness. Ekkad et al. (1995) reported film cooling effectiveness results for compound angle holes with relatively high turbulence intensity and found that higher density injectant tends to result in a higher film cooling effectiveness for simple injection, while lower density coolant results in a higher effectiveness for a large compound angle.

Jubran and Brown (1985) reported the effect of favorable pressure gradients on film cooling from simple angle injection holes. It was concluded that a moderate favorable pressure gradient tends to reduce the value of the average film cooling effectiveness downstream of the injection holes. Teekarama et al. (1991) studied experimentally film cooling in the presence of mainstream pressure gradient on a flat plate downstream of an inclined slot and a single row of holes in the presence of favorable and adverse pressure gradients. They found that an accelerating flow tends to increase film cooling effectiveness over that for zero or adverse pressure gradients. Ammari et al. (1991) investigated the effect of an accelerating flow on the heat transfer coefficient on a film-cooled surface. It was reported that the heat transfer coefficient under the film is decreased as the acceleration is increased.

It appears from the aforementioned investigations and the other numerous investigations carried out on film cooling from simple angle holes that no attempt was made to investigate the effects of mainstream turbulence or pressure gradient on film cooling and heat transfer over a flat plate using a row of simple angle holes in combination with a row of compound angle holes. Furthermore, this paper attempts to correlate the film cooling results from combination of two rows injection models using a two-dimensional correlation group.

2. Experimental apparatus and measuring system

The experimental investigation was conducted in an open suction-type wind tunnel with a square cross-section area of 30 cm × 30 cm and of length equal to 200 cm, Fig. 1. The wind tunnel is capable of providing a uniform free stream at a controlled velocity up to 40 m/s. The boundary layer was tripped along the middle of the bottom side of the test section

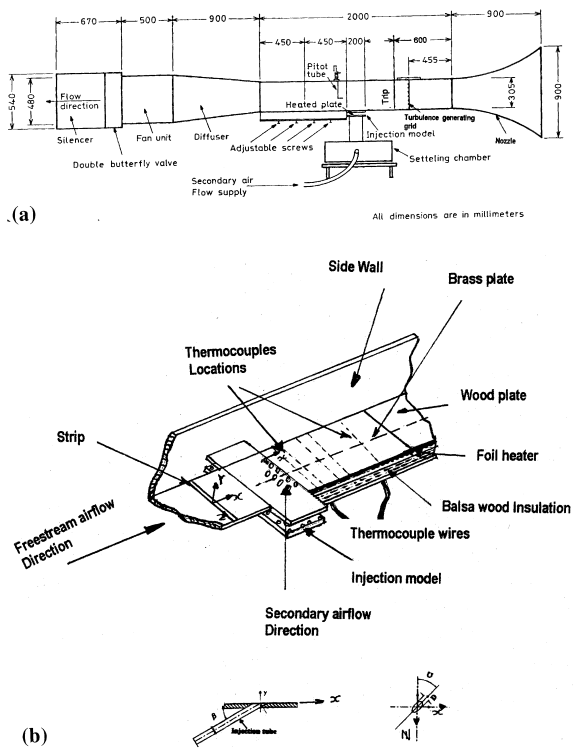

Fig. 1. (a) Schematic diagram of the experimental rig. (b) Details of the test section and injection tube angles.

at a distance 30 cm upstream from the leading edge of the first row of holes with a 1.5 mm high strip of tape. The boundary layer thickness to the injection-hole diameter ratio is 0.99. The various pressure gradients were obtained by tilting the roof of the test section either to form a nozzle like arrangement or a diffuser like arrangement with the bottom test surface plate, to obtain favorable or adverse pressure gradients, respectively. One pressure gradient over the test section was obtained for each tilt angle of the roof. The pressure gradient factors are in the range -1.11×10^{-6} to $+1.11 \times 10^{-6}$. When the turbulence generating grid was not employed, the freestream turbulence intensity at the mid section is 0.3%. In order to simulate the turbulence intensity which occurs in a practical situation in gas turbines, a grid consisting of a row of parallel bars were used and clamped at the entry of the working section, to increase the mainstream turbulence intensity. The design of the turbulence grid was based on the work of Rose (1970), who used a similar arrangement to obtain a homogeneous form of turbulence. Rose reported, that provided the diameter of the bar is greater than 3 mm, the turbulence will increase as the ratio of the bar diameter to the distance between them increased. The turbulence intensity at the injection point at the mid section generated in the present investigation is 4.7%. The freestream air was maintained at ambient temperature. Hot air was injected through the base of the working section. A summary of the experimental conditions is shown in Table 1.

The injection configurations investigated included eight models, each consisted of two rows of holes arranged in either staggered or in-line arrangements of either both rows having compound angle holes or both rows having simple angle holes or combinations of one row of simple angle holes and the other row of compound angle holes, all holes were 13 mm diameter. Both compound and simple-angle holes were inclined at $\Omega = 35°$ with respect to the test surface when projected into the streamwise/normal plane. The compound-angle holes were

Table 1
Summary of experimental conditions

P/D	2.0
S/D	2.31
Freestream velocity	10 m/s
Turbulence Intensity (Tu)	0.3–4.7%
Pressure gradient factor (K)	-1.11×10^{-6} to $+1.11 \times 10^{-6}$
Freestream temperature	9–14°C
Reynolds number based on the length from the leading edge of the first row of holes to the end of the heated surface	2.1×10^5–4.9×10^5
Reynolds number of coolant flow based on injection hole diameter	0.913×10^3–5.475×10^3
δ/D	0.99
δ^*/D	0.096
Nondimensional injection temperatures	0.0–3.0

additionally inclined at $\beta = 30°$ when projected into the spanwise/normal plane, a summary of the injection models is shown in Table 2.

The heat transfer surface was designed and built to provide a constant heat flux over the test plate. The plate was made such that its upper surface is facing the wind tunnel air stream, with minimal conduction heat losses from the side and bottom of the test surface. The test surface next to the injection holes is made of polished brass of 3 mm thickness. Immediately beneath this, is a liner containing 65 thermocouples located at 1 mm below the upper surface of the polished brass where the wires are passed through grooves in the lower side of the brass plate. The grooves were then filled with RTV epoxy, which has high thermal conductivity. The 65 copper–constantan thermocouples were located in six rows over the test plate. In each of the six rows, 11 thermocouples were located 1 cm apart.

A thin foil heater, 28 cm × 43 cm × 0.3 cm, rated at 235 V and 700 W was used to heat the test surface plate, and immediately below the heater a 100 mm thick piece of balsa wood was located to minimize the heat losses from the bottom surface of the heater. The surface temperature was controlled by adjusting the input voltage to the heater using a standard variac. The injectant flow was heated above the ambient temperature using a four-coil heater. Each heater is capable of producing 800 W and rated at 220 V. The coils are wired such that three of them can be operated at either zero or full power, and one of them can be operated over a continuous range from zero to full power with the assistance of a variac. Such arrangements would enable the input heat to vary between zero and 3200 W.

Copper–constantan thermocouples were used to measure temperatures along the surface of the test plate and in the spanwise direction at various locations downstream of the holes, the freestream temperature, settling chamber and the exit of injection holes temperatures. The thermocouples from the heated surface were connected to a 3530 Orion data logging system.

Table 2
Injection models specifications

Model	Upstream row/Downstream row	Arrangement of rows
A	Compound/compound	Inline
B	Compound/compound	Staggered
C	Simple/compound	Inline
D	Compound/simple	Inline
E	Simple/compound	Staggared
F	Compound/simple	Staggered
G	Simple/simple	Inline
H	Simple/simple	Staggered

3. Data reduction

The rate of the convective heat transfer that is released from the plate is given by

$$q = q_{\text{total}} - \Delta q, \tag{1}$$

where q_{total} is the power supplied to the plate and the term Δq is a small correction made up from a conduction loss Δq_{cond} and a radiation loss Δq_{rad}. Introducing the conduction and radiation losses to Eq. (1), the convective heat transfer from the heated plate is given by

$$q = q_{\text{total}} - \Delta q_{\text{cond}} - \Delta q_{\text{rad}}. \tag{2}$$

The heat loss by conduction is obtained by insulating the top of the test surface (which is usually exposed to the mainstream) and measuring the conduction losses from the bottom as it is dependent upon the difference in temperatures between the test surface and the surrounding ambient air. Radiation losses from the top of the test surface were analytically estimated. For an average plate temperature of 25°C with a freestream velocity of 10 m/s and 14°C, radiation losses were approximately 1.0 W or about 0.34% of the total power into the test plate.

The fraction of the known power supplied to the plate, which contributes to the convective heat transfer from the plate, was calculated from Eq. (2) as

$$q = EI - \frac{1}{R_{\text{cond}}}(T_{\text{w}} - T_{\infty}) - \varepsilon\sigma A_{\text{s}}(T_{\text{w}}^4 - T_{\infty}^4), \tag{3}$$

where E the voltage drop across the heater, I the current passing through the heater, R_{cond} the thermal conduction resistance, ε the emissivity of the plate, σ the Stefan–Boltzmann constant, A_{s} the exposed surface area of the test plate, T_{w} the wall temperature and T_{∞} the freestream temperature.

Adiabatic film cooling effectiveness was determined using the linear superposition theory applied to Stanton number ratios measured at different injection temperatures. The technique of superposition was first applied to film cooling by Metzger et al. (1968). Eckert et al. (1977) showed how local heat transfer coefficient ratios for different injection temperatures can be deduced from the adiabatic wall temperature, T_{aw} and the iso-energetic heat transfer coefficient, h_{f}. The heat flux with film cooling is found from

$$q = h_{\text{f}}(T_{\text{w}} - T_{\text{aw}}). \tag{4}$$

This is also given by

$$q = h(T_{\text{w}} - T_{\text{r},\infty}). \tag{5}$$

Solving Eqs. (4) and (5) leads to

$$h = h_{\text{f}}(1 - \eta\theta), \tag{6}$$

where $\theta = (T_{\text{r,c}} - T_{\text{r},\infty})/(T_{\text{w}} - T_{\text{r},\infty})$ and $\eta = (T_{\text{aw}} - T_{\text{r},\infty})/(T_{\text{r,c}} - T_{\text{r},\infty})$. Dividing Eq. (6) by h_{o}, the heat transfer coefficient in terms of Stanton number is obtained from

$$\text{St}/\text{St}_{\text{o}} = \text{St}_{\text{f}}/\text{St}_{\text{o}}(1 - \eta\theta). \tag{7}$$

The local film cooling measurements were used to find the spanwise averaged adiabatic film cooling effectiveness, which is given by

$$\bar{\eta} = \frac{1}{L}\int_0^L \eta \, dz. \tag{8}$$

The spanwise averaged iso-energetic Stanton number ratio is given by

$$\frac{\overline{St_f}}{St_o} = \frac{1}{L}\int_0^L \frac{St_f}{St_o} dz, \tag{9}$$

where L is the length of the test surface in the spanwise direction.

4. Results and discussion

Throughout the measurements made to establish the data presented in this article, care was taken to note possible sources of error and an error analysis based on the method of Kline and McClintock (1953). The error analysis indicated an error of ±5% uncertainty in the film cooling measurements. The maximum errors in the calculation of the heat transfer (h) and the St/St_o were ±3.8% and ±5.3%, respectively. The uncertainty in the coolant flux ($\rho_c U_c$) was ±3%.

Fig. 2 shows a comparison of η for six hole arrangements of injection models investigated, as outlined in Table 2 for low blowing rate, $M = 0.2$ at the vicinity of the injection models at $x/D = 2.96$. This figure indicates clearly that model E (simple angle injection hole for the upstream row and compound angle hole for the downstream row) tends to give better cooling protection than the rest of injection models investigated as can be seen from the η values obtained. Furthermore, the figure shows that the staggered compound angle injection model B tends to give a slightly better cooling protection than the inline compound injection model A.

When inline arrangements were used with two rows of one compound and one simple angle hole rows in combinations, models C and D, both models give the lowest film cooling effectiveness when compared with other models. However, when the simple angle holes injection row is located downstream for the inline injection arrangement (model D) it gives a significant increase in the film cooling effectiveness over that when the simple injection row is located upstream, (model C). The effect of using a combination of a simple angle holes row with a compound angle holes row in a staggered arrangement is shown in the same Fig. 2 for models E and F. The results indicate that better cooling protection is obtained when the simple injection row is located upstream, model E. Fig. 3 shows the same comparison as in Fig. 2 but for higher blowing rate, $M = 0.5$. Similar findings were found to that at low blowing rate, $M = 0.2$, but with an increase in the local film cooling effectiveness.

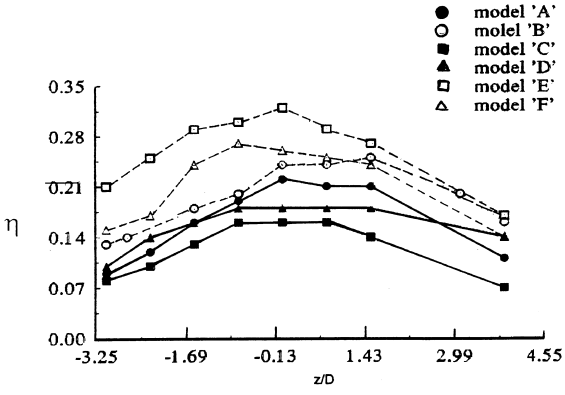

Fig. 2. Comparison of the local variation of adiabatic film cooling effectiveness at $x/D = 2.96$ with $M = 0.2$ for various injection models.

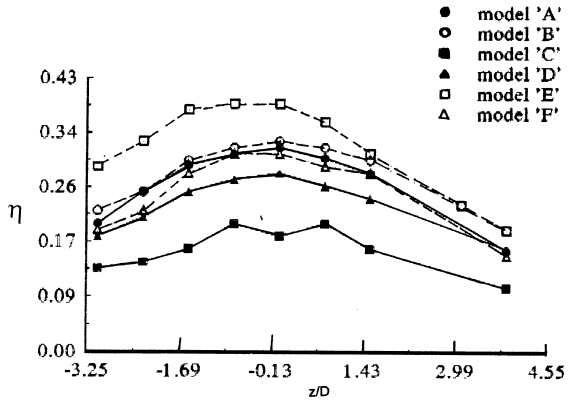

Fig. 3. Comparison of the local variation of adiabatic film cooling effectiveness at $x/D = 2.96$ with $M = 0.5$ for various injection models.

It has been known for some time that pressure gradients have some influence on film cooling from simple angle injection holes but not much is said regarding such effects on film cooling from compound injection holes or combinations of simple and compound injection holes rows. Figs. 4 and 5 show the effect of favourable and adverse pressure gradients on one injection model with both rows having compound angle holes, model B and on an injection model having one row of simple angle holes upstream and one row of compound angle holes at the downstream row, model E for $M = 0.2$ and 0.6. These figures indicate that the favourable pressure gradient reduces the local film cooling effectiveness for both blowing rates of model B while for model E the effect is only significant at low blowing rate.

The effect of adverse pressure gradient for both models B and E is shown again in Figs. 4 and 5 which indicate that the effect is very much dependent on the blowing rate. For models

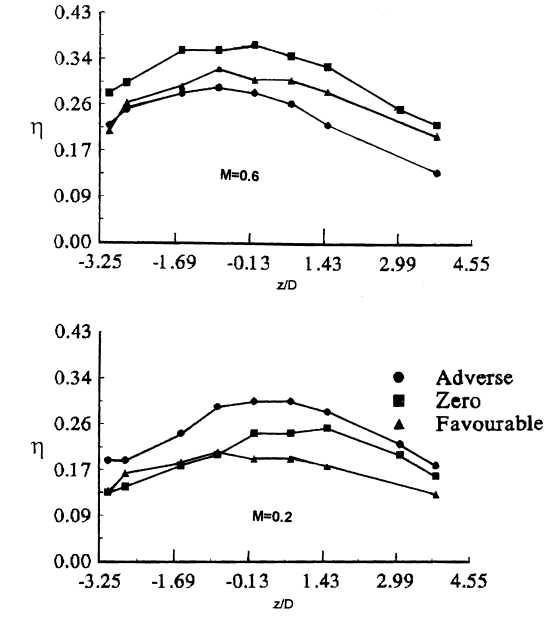

Fig. 4. Effect of pressure gradients on the local adiabatic film cooling effectiveness at $x/D = 2.96$ for model B for $M = 0.2$ and 0.6.

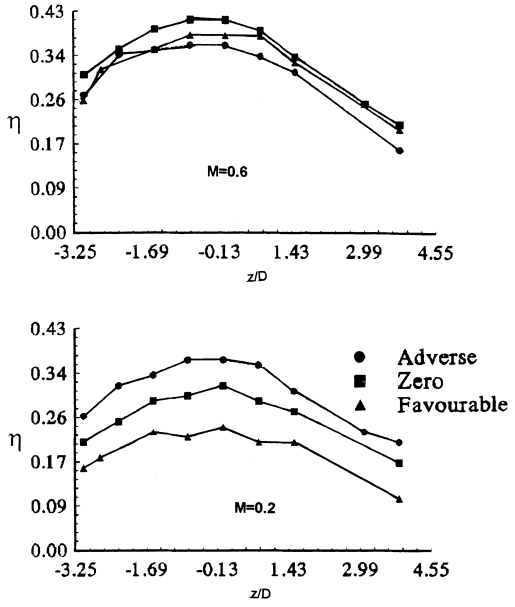

Fig. 5. Effect of pressure gradients on the local adiabatic film cooling effectiveness at $x/D = 2.96$ for model E for $M = 0.2$ and 0.6.

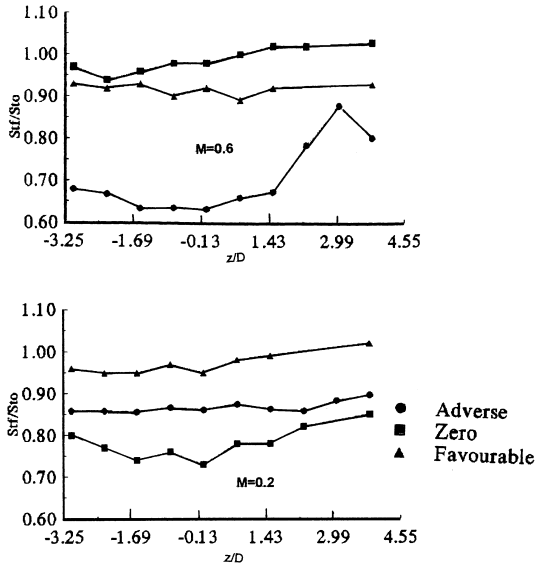

Fig. 7. Effect of pressure gradients on the local iso-energetic Stanton number ratio at $x/D = 2.96$ for model E for $M = 0.2$ and 0.6.

B and E at $x/D = 2.96$, the adverse pressure gradient increases the film cooling effectiveness at $M = 0.2$ while reducing it at high blowing rate $M = 0.6$. Liess (1974), Jubran and Brown (1985) and Teekaram et al. (1991) reported similar trends to the film cooling results reported here for pressure gradient effects on compound angle holes but using simple angle holes injections.

The effect of pressure gradients on the average film cooling effectiveness for model B is shown in Fig. 6 for $M = 0.2$ and 0.6. The favorable pressure gradient decreases the average film cooling effectiveness, which is more significant for high blowing rate. The adverse pressure gradients effect on average film cooling effectiveness using model B tends to increase the average film cooling effectiveness slightly at $M = 0.2$ but results in a significant reduction at $M = 0.6$.

The local variations of the iso-energetic Stanton number ratio at the vicinity of the injection holes, $x/D = 2.96$ for the combination rows (model E) at $M = 0.2$ and 0.6 with zero, adverse and favorable pressure gradients are plotted in Fig. 7. The figure indicates clearly that at low blowing rate, $M = 0.2$ both adverse and favorable pressure gradients increase the St_f/St_o but with the favorable pressure gradient the effect is more severe. At high blowing rate the effect is reversed where both pressure gradients tend to reduce the St_f/St_o.

The effect of pressure gradients on the spanwise-average iso-energetic Stanton number ratio, $\overline{St_f/St_o}$ for model E is shown in Fig. 8. Again, both gradients increase the $\overline{St_f/St_o}$ at

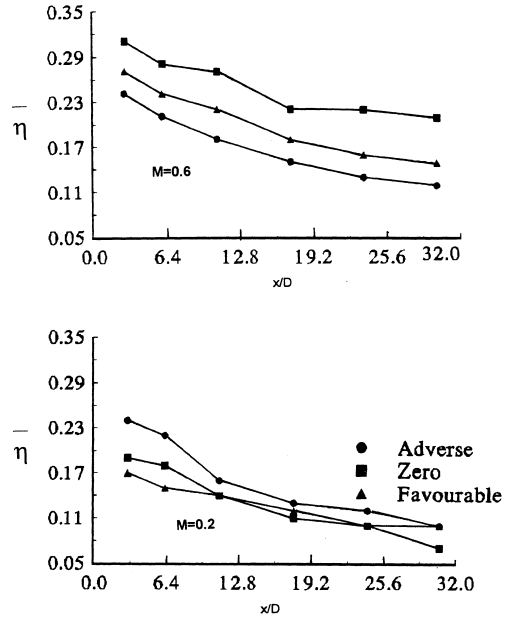

Fig. 6. Effect of pressure gradients on the spanwise-average film cooling effectiveness for model B for $M = 0.2$ and 0.6.

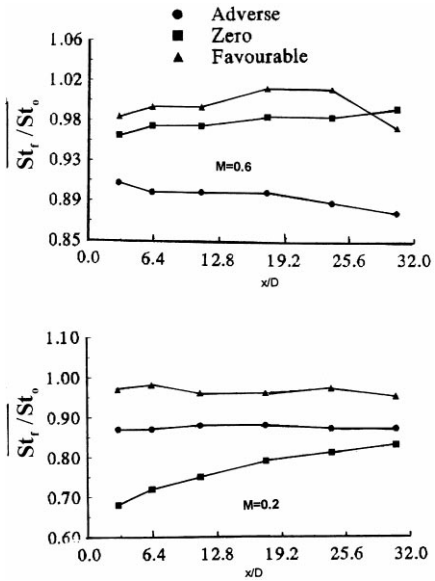

Fig. 8. Effect of pressure gradients on the spanwise average iso-energetic Stanton number ratio for model E for $M = 0.2$ and 0.6.

$M = 0.2$. However, the effect of adverse pressure gradient diminishes and the favourable pressure gradient effects is increased at $M = 0.6$ for all distances of x/D.

The effects of free stream turbulence intensity generated upstream of the injection holes on the local and average film cooling effectiveness for blowing rate, $M = 0.2$ and 0.6 are shown in Figs. 9 and 10. These figures indicate clearly that for the combination models used, increasing the turbulence reduces both the local and average film cooling effectiveness in the vicinity of the holes, $x/D = 2.96$ and further downstream at $x/D = 30.6$ for low and high blowing rates. In general, increasing turbulence intensity tends to decrease film cooling effectiveness though the effect on the lateral averaged effectiveness is smaller than the one on the local effectiveness. These findings agree with results obtained for simple angle holes such as those reported by Launder and York (1974) and Brown and Minty (1975). The effect of increasing the turbulence intensity on the heat transfer ratio $\overline{St_f/St_o}$ is very much dependent on the blowing rate while at low blowing rate $M = 0.2$ it tends to increase the heat transfer ratio, at high blowing rate, $M = 0.6$ this is true only at the vicinity of the injection holes. At $x/D > 12.8$ the increase in turbulence reduces the heat transfer ratio with the distance downstream, Fig. 11.

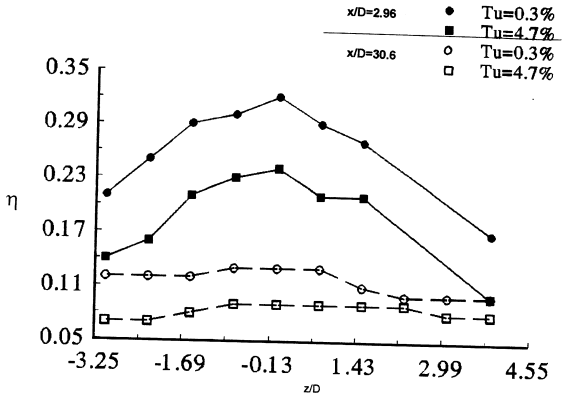

Fig. 9. Effect of turbulence intensity on the local adiabatic film cooling effectiveness at various distances downstream for model E for $M = 0.2$.

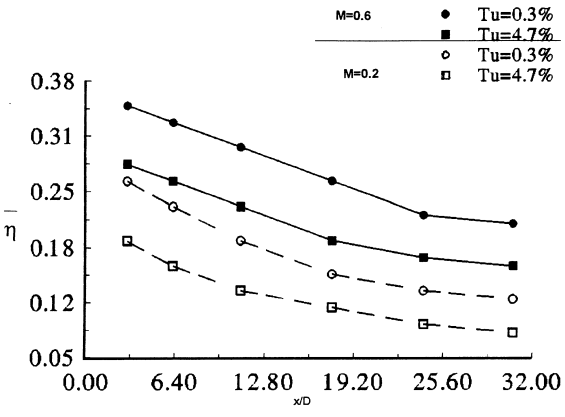

Fig. 10. Effect of turbulence intensity on the spanwise-average film cooling effectiveness for model E for $M = 0.2$ and 0.6.

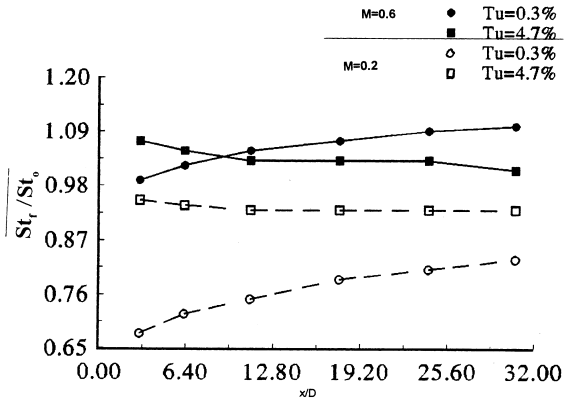

Fig. 11. Effect of turbulence intensity on the spanwise-average isoenergetic Stanton number ratio for model E for $M = 0.2$ and 0.6.

5. Correlations of film cooling

The correlations of the average film cooling effectiveness downstream of two rows of injection holes having different hole angles and arrangements are examined for six injection models A, B, C, D, E, and F, and for five blowing rates $M = 0.2$–0.6. Brown (1967) developed correlation groups based on a heat balance model for a two-dimensional model and suggested that the following group is useful,

$$A = (Ms/x)(\mathrm{Re}_x)^{0.5}/(1 - x_i/x), \tag{10}$$

where x is the distance from the leading edge of the test plate and x_i the distance up to the injection point. Brown further found that introducing the momentum ratio I into the correlation groups caused the effectiveness measurements to collapse into a single curve for a given injection angle in the streamwise direction and for all low blowing rates and another curve for all high blowing rates. This led to the following correlation,

$$\eta = f_1(I) f_2(A), \tag{11}$$

where $f_2(A, I) = A^{\gamma}$ and $\gamma = f_3(I)$. The value of s used in the present investigation for group A is the equivalent slit width of area equal to the area of the holes through which the coolant was injected, that is, $s = (\pi D^2/4P)$. Eqs. (10) and (11) have been applied with some success to effectiveness measurements for a single row of simple angle holes (Brown and Saluja, 1979) and for two rows of simple angle holes (Jubran, 1989).

Using the same group of correlations for the averaged film cooling effectiveness from compound angle holes models and combination injection models as that used for simple angle holes, the following correlations are obtained for the various models investigated with typical correlation for low blowing rates shown in Fig. 12.

Correlations for model A at low and high blowing rates, respectively:

$$\overline{\eta} = 0.0118 I^{2.39} A^{0.932 I^{-0.464}}, \tag{12}$$

$$\overline{\eta} = 0.033 I^{0.544} A^{0.393 I^{-0.466}}. \tag{13}$$

Correlations for model B at low and high blowing rates, respectively:

$$\overline{\eta} = 0.0017 I^{0.702} A^{0.102 I^{-0.236}}, \tag{14}$$

$$\overline{\eta} = 0.0874 I^{0.198} A^{0.26 I^{-0.484}}. \tag{15}$$

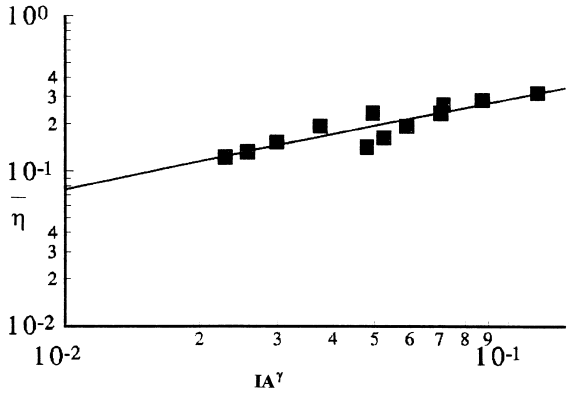

Fig. 12. Typical correlation for the average film cooling effectiveness of model E at low blowing rates ranges.

Correlations for model C at low and high blowing rates, respectively:

$$\overline{\eta} = 0.0239 I^{0.825} A^{0.373 I^{-0.869}}, \tag{16}$$

$$\overline{\eta} = 0.075 I^{0.55} A^{0.12 I^{-0.198}}. \tag{17}$$

Correlations for model D at low and high blowing rates, respectively:

$$\overline{\eta} = 0.0078 I^{0.752} A^{0.655 I^{-0.724}}, \tag{18}$$

$$\overline{\eta} = 0.0071 I^{0.421} A^{0.328 I^{-0.197}}. \tag{19}$$

Correlations for model E at low and high blowing rates, respectively:

$$\overline{\eta} = 0.0166 I^{0.624} A^{1.01 I^{-0.36}}, \tag{20}$$

$$\overline{\eta} = 0.0466 I^{0.258} A^{0.41 I^{-0.381}}. \tag{21}$$

Correlations for model F at low and high blowing rates, respectively:

$$\overline{\eta} = 0.0022 I^{1.484} A^{1.31 I^{-0.723}}, \tag{22}$$

$$\overline{\eta} = 0.049 I^{0.503} A^{0.354 I^{-0.516}} \tag{23}$$

when the correlation results for all models investigated were plotted as shown for a typical injection model in Fig. 12. The two dimensional correlation groups presented in this section tends to give better correlations when used for combination injection models and high blowing rates than when used for the compound injection models and low blowing rate. The accuracy of the correlations for the other models and blowing rates not shown here is in the range of 5–15%.

6. Conclusions

The following points emerged from the present investigation:

1. The effect of favorable pressure gradients is to reduce the local film cooling from two rows of holes with compound angle holes at both rows or combination of one row of simple angle holes and one row of compound angle holes. The significance of this effect is dependent on the blowing rate especially for the combination angle holes model.

2. The effect of adverse pressure gradient for injection models of only compound angle holes or combination of simple and compound angle holes rows is very much dependent on the blowing rate where it tends to increase the film cooling effectiveness at low blowing rate but reduces the film cooling at high blowing rate.

3. High freestream turbulence intensity results in a reduction in both the local and average film cooling effectiveness from injection models with combination of compound and simple injection holes rows. However, such an effect is more significant on a particular local film cooling effectiveness.

4. The averaged film cooling effectiveness from an injection model of either two rows of compound angle holes or one row of compound angle holes and one simple angle holes row can be correlated by using a two dimensional film cooling correlation provided that the momentum ratio I is incorporated in the correlation.

References

Ammari, H.D., Hay, N., Lampard, D., 1991. Effect of acceleration on the heat transfer coefficient on a film cooled surface. ASME Journal of Turbomachinery 113, 464–471.

Bons, J.P., MacArthur, C.D., Rivir, R.B., 1996. The effect of high freestream turbulence on film cooling effectiveness. ASME Journal of Turbomachinery 118, 814–825.

Brown, A., 1967. Theoretical and experimental investigation into film cooling. JSME 1967 Semi-International Symposium, Tokyo, pp. 199–211.

Brown, A., Minty, A.G., 1975. The effects of mainstream turbulence intensity and pressure gradient on film cooling effectiveness for cold air injection slits of various aspect ratios. ASME 75-WA-17.

Brown, A., Saluja, G.L., 1979. Film cooling from a single hole and a row of holes of variable pitch to diameter ratio. Int. J. Heat and Mass Transfer 22, 525–533.

Ekkad, S.V., Zapta, D., Han, J., 1995. Film cooling over a flat surface with air and CO_2 injection through compound angle holes using a transient liquid crystal image method. ASME paper 95-GT-11.

Eckert, E.R.G., Pederson, D.R., Goldstein, R.J., 1977. Film cooling with large density differences between the mainstream and the secondary fluid measured by the heat mass transfer analogy. ASME Journal of Heat Transfer 99, 620–627.

Jubran, B.A., 1989. Correlations and prediction of film cooling from two rows of holes. ASME Journal of Turbomachinery 111, 502–509.

Jubran, B., Brown, A., 1985. Film cooling from two rows of holes inclined in the streamwise and spanwise directions. ASME Journal of Engineering for Gas Turbines and Power 107, 84–91.

Jumper, G.W., Elrod, W.C., Rivir, R.B., 1991. Film cooling effectiveness in high-turbulence flow. ASME Journal of Turbomachinery 113, 479–483.

Kline, S.J., McClintock, F.A., 1953. Describing uncertainties in single sample experiments. Mechanical Engineering 75, 3–8.

Launder, B.E., York, J., 1974. Discrete hole cooling in the presence of free stream turbulence and strong favorable pressure gradient. Int. J. Heat and Mass transfer 17, 1403–1409.

Ligrani, P.M., Mitchell, S.W., 1994. Interaction between embedded vortices and injectant from film cooling holes with compound angle orientations in a turbulent boundary layer. ASME Journal of Turbomachinery 116, 80–91.

Liess, C., 1974. Experimental investigation of film cooling with ejection from a row of holes for the application to gas turbine blades. ASME Paper 74-GT-5.

Mehendale, A.B., Han, J.C., 1992. Influence of high mainstream turbulence on leadinf edge film cooling heat transfer. ASME Journal of Turbomachinery 114, 707–715.

Metzger, D.E., Carper, H.J., Swank, L.R., 1968. Heat transfer with film cooling near nontangential injection slots. ASME Journal of. Engineering for Power 90, 157–163.

Rose, W.G., 1970. Interaction of grid turbulence with a uniform mean shear. Journal of Fluid Mechanics 44, 767–779.

Schmidt, D.L., Sen, B., Bogard, D.G., 1996. Film cooling with compound angle holes: adiabatic effectiveness. ASME Journal of Turbomachinery 118, 807–813.

Teekarama, A.J.H., Forth, C.J.P., Jones, T.V., 1991. Film cooling in the presence of mainstream pressure gradients. ASME Journal of Turbomachinery 113, 484–492.